Drivers and uncertainty of Amazon carbon sink long-term and interannual variability in CMIP6 models

Matteo Mastropierro[1], Daniele Peano[2], Davide Zanchettin[1]

[1] Department of Environmental Sciences, Statistics and informatics, Ca' Foscari University of Venice, Venice, Italy
[2] CMCC Foundation - Euro-Mediterranean Center on Climate Change, Bologna, Italy.

Correspondence to: Matteo Mastropierro (matteo.mastropierro@unive.it)

Abstract. The Amazon basin rainforest is a critical component of the climate system, currently representing 25% of terrestrial carbon gains and storing 150 to 200 billion tonnes of carbon. Whether the Amazon rainforest will remain a net carbon sink is an open scientific question: while its future stability and functioning may be compromised by climate change and anthropogenic pressures, Earth System Models (ESM) divergence in the projections undermines their reliability to simulate its future evolution. In this study, we examined the contribution of different climatic drivers behind the long-term and interannual variability evolution of the carbon sink within the Amazon basin using eleven CMIP6 ESMs, shedding light on the main factors contributing to inter-model diversity. By adopting the carbon-cycle feedback framework with C4MIP experiments, our results underscore the dominant role of CO_2 fertilization in driving long-term Amazon carbon sink trend and uncertainty. We also address the variability of carbon fluxes at the interannual timescale using a multivariate predictive model on historical and ssp585 ScenarioMIP simulations. With this respect, we emphasize the contribution of GPP modulation by shortwave incoming radiation as dominating NBP divergence across the ESMs ensemble. Additionally, we demonstrate that temperature-driven anomalies will be the main mechanism responsible for the higher Amazon carbon sink sensitivity to the El Nino Southern Oscillation (ENSO) under sustained global warming, predominantly as a result of the amplification of NBP sensitivity to temperature anomalies. Being the representation of terrestrial carbon cycle processes still one of the main uncertainties undermining ESMs projections, we therefore advocate for increased focus from modelling groups towards a more accurate and consistent representation of land processes and parameterizations, which will hopefully lead to reduced uncertainties in simulations coming from the next generation of ESMs.

1 Introduction

The Amazon basin rainforest plays a fundamental role in the climate system, serving as a prominent actor in the land carbon cycle and by exerting a significative influence on the global energy budget and hydrological cycle (Davidson et al., 2012). At the same time, the land carbon sink represents one of the crucial uncertainties affecting climate change future evolution (Canadell et al., 2021; Friedlingstein et al., 2006; K. Arora et al., 2020). Indeed, projections of the Amazon climate and carbon sink are still poorly constrained by state-of-the-art Earth System Models (ESMs), indicative of persisting gaps of knowledge regarding this critical aspect of the Earth system (Ahlström et al., 2012; Baker et al., 2021; Koch et al., 2021a; Lin et al., 2023; Raoult et al., 2023; Xu et al., 2020; Zhu et al., 2019).

The Amazon ecosystem has been a long-term carbon sink during the past decades contributing to approximately 25% of terrestrial carbon gains, estimated in 0.42-0.65 Gt C yr^{-1} for the period 1990–2007, a trend mainly driven since the 1980s by the CO_2 fertilization effect from rising CO_2 concentrations in the atmosphere (O'Sullivan et al., 2019; Pan et al., 2011; Phillips et al., 2009; Walker et al., 2021). Nevertheless, recent estimates have demonstrated a slow-down of net carbon sequestration and consequently a saturation and declining trend in the Amazon carbon sink, with increase in carbon losses due to drought events and increased temperatures (Brienen et al., 2015; Hubau et al., 2020). Both CO_2 concentrations in the atmosphere and climatic conditions affect land carbon fluxes. Higher atmospheric CO_2 concentrations exert mainly a positive direct effect on photosynthesis through plants stomatal closure and the associated negative Carbon-Concentration feedback (Boer and Arora, 2009; K. Arora et al., 2020), while they can indirectly increase Ra and Rh (Gao et al., 2020). Climatic conditions, on the other hand, mainly affect vegetation carbon fluxes through temperature and water availability, with, for example, negative temperature impacts on primary productivity and a positive (negative) relationship between temperature (water availability) and changes in respiration rates (Canadell et al., 2021; Gentine et al., 2019; Green et al., 2019; Humphrey et al., 2018; Liu et al., 2020). With this respect, interannual variations of water availability and temperature in the Amazon basin are mainly related to El Niño-Southern Oscillation (ENSO), which is responsible for a vast part of the climatological and net land CO_2 fluxes variability observed in tropical biomes (Bastos et al., 2018; Jones et al., 2001; Kim et al., 2016; Mcphaden et al., 2021a; Piao et al., 2020; Zhu et al., 2017). Accordingly, some of the most severe droughts observed in the Amazon basin in recent decades and the associated reduction of the net land CO_2 sink were forced by strong ENSO events (or El Niños), most prominently the 1997/1998 and 2015/2016 ones (Jiménez-Muñoz et al., 2016; Koren et al., 2018; Liu et al., 2017). Despite indications of temperature-driven GPP anomalies were responsible for decreased Amazonian carbon sink in the 2015/2016 event (Bastos et al., 2018; Zhang et al., 2019), it is still currently debated whether fluctuations in temperatures or water availability are the dominant drivers for interannual carbon variability of tropical biomes, with recent research indicating the increased importance of water availability as a controlling factor in the past decades and with ESMs failing to reproduce this observed behavior (Humphrey et al., 2018; Jung et al., 2017; Liu et al., 2023; Zhang et al., 2023).

Consequently, at least three factors will contribute to determining whether, and to which extent, the Amazon ecosystem will remain a net carbon sink in the future decades under sustained positive radiative forcing: mean-state climatic changes, nutrient

limitation, and ENSO modulation. First, a significant increase in surface air temperature and a marked decline in water availability in the Amazon basin deriving from increased greenhouse gas emission scenarios will most likely result in a less effective carbon sink by the end of the 21st century . In particular, coupled climate models suggest that the reduction in precipitation is driven by reduced evapotranspiration resulting from stomatal closure response to increased CO_2, which lead to changes in local surface energy balance and atmospheric circulation patterns (Kimm et al., 2024; Kooperman et al., 2018; Langenbrunner et al., 2019; Li et al., 2023). Then, Nitrogen and Phosphorous will likely limit tropical forests productivity (Fleischer et al., 2019), an effect partly counterbalanced by the positive influence exerted by the increasing atmospheric CO_2 concentrations (Huntingford et al., 2013; Koch et al., 2021b). Lastly, an increased Amazon vegetation sensitivity to ENSO is expected under a range of global warming scenarios (Kim et al., 2017; Park et al., 2020; Uribe et al., 2023). In particular, global warming could affect the ENSO-Amazon teleconnection either from changes in mean-state and extremes in ENSO cycle, or from variations in the ENSO teleconnection mechanism itself (Beobide-Arsuaga et al., 2021; Cai et al., 2021; Chen et al., 2017; Mcphaden et al., 2021c; Yeh et al., 2018; Zheng et al., 2017). Notably, ENSO amplitude is slightly yet significantly enhanced under future global warming scenarios (Beobide-Arsuaga et al., 2021; Cai et al., 2022), and regional patterns of precipitation and temperature anomalies over South America associated with ENSO teleconnections are projected to be amplified in warmer climates (McGregor et al., 2022; Perry et al., 2020).

Given these premises, in this research we investigate the Amazon carbon sink using coupled simulations from CMIP6 ESMs simulations (Eyring et al., 2016; O'Neill et al., 2016) to separate the relative contributions of long-term changes and interannual variability under sustained atmospheric CO_2 concentrations and global warming. Specifically, throughout the paper, two question that remains underexplored in the literature are tackled: what are the relative contributions of inter-annual variability (IAV) and long-term climatic changes in the projected Amazon net carbon sink evolution? What is the role of ENSO in exerting a control on temperature and water availability? In doing that, an attempt is performed to identify the factors contributing to inter-model diversity in Amazon vegetation productivity projections across the ESMs considered.

2 Data and Methods

2.1 Data

We use simulations from eleven CMIP6 generation ESMs that contributed to both C4MIP and ScenarioMIP projects (Eyring et al., 2016; Jones et al., 2016; O'Neill et al., 2016). In particular, the following experiments have been considered: 1pctCO2-bgc, 1pctCO2-rad, ssp585-bgc, ssp585-rad, historical and ssp585. ScenarioMIP simulations (historical and ssp585) aim to reproduce the climatic response to realistic forcing of the historical period and to a prescribed 8.5 W/m² radiative forcing increase by the end of the 21st century. C4MIP experiments (1pctCO2-bgc, 1pctCO2-rad, ssp585-bgc, ssp585-rad) are idealized concentration-driven carbon-climate simulations generated to better understand and quantify changes in the ocean and land carbon storage and fluxes under different climatic conditions. Specifically, the experiments aim to test the carbon cycle

response to the effect of increased CO_2 concentrations in the atmosphere (-bgc simulations) and increased radiative forcing resulting from higher atmospheric CO_2 concentrations affecting the climate system (-rad simulations). These two categories of simulations differ in their model set-up, so that in the former (-bgc), only the model land and ocean carbon cycle respond to a CO_2 increase while the radiation scheme uses a preindustrial CO_2 concentration, therefore allowing to test the biogeochemical effect of atmospheric carbon dioxide increase without the associated radiative forcing. Reversely, in -rad simulations the biogeochemical effect is factored out, hence the climate responds to the radiative forcing by increased CO_2 concentration, whereas the carbon cycle remains constrained by a preindustrial atmospheric CO_2 level. In our analysis, we adopt C4MIP simulations forced either with a 1 % per year increase in atmospheric CO_2 concentrations up to four times the preindustrial level of 280 ppm, with no confounding effect of changes in land use, non-CO_2 greenhouse gases, and aerosols, or with a standard CO_2 pathway from the ssp585 scenario. For the sake of our goal, we count these differences negligible, as considering both 1pctCO2 and ssp585 experiments allows us to have a higher ensemble of data available.

Those ESMs for which at least one realization is available for all the simulation experiments and that have all the prognostic variables needed for the analysis available (or computable indirectly) have been included in the research. Table 1 presents an overview of the experiments considered and the methodologies adopted for each experiment. For the historical and ssp585 experiments, specifically, the first five realizations of each model (when more than one was available) were used to account for the uncertainty stemming from internal climatic variability, with the caution of having the same simulation members for the historical and ssp585 scenarios to make a pairwise comparison. The details of the ESMs used are reported in Table SI1. For these historical and ssp585 simulations, the analyses have been performed on single realizations, and aggregated by model solely for the graphical presentation of the results. The evolution of the land carbon-cycle is investigated by considering long-term changes and interannual variability of NBP values, which represent the balance of Gross Primary Productivity (GPP) due to photosynthesis at the net of autotrophic respiration (Ra), heterotrophic respiration (Rh) and disturbances, as fire dynamics (for those model having a fire module) and Land Use Change (LUC). Overall, the following variables have been considered in the study: sea-surface temperature (SST), Net Biome Productivity (NBP), Gross Primary Production (GPP), autotrophic respiration (Ra), heterotrophic respiration (Rh) , precipitation (Pr), soil moisture (mrso), air surface temperature (T) and shortwave incoming radiation (SWin).

Table 1: Overview of the experiments and methodologies used in the research. We refer to the work of Jones et al., **(2016)** and O'Neill et al., **(2016)** for more information on the C4MIP and ScenarioMIP experiments reported in this table.

Project	Experiments	Reference years	ESMs (n°)	Coupling	Effect estimated
C4MIP	1pctCO2-rad	36-150	11	Radiative-only	Long-term, Climate
	ssp585-rad	2015-2100	7	Radiative-only	Long-term, Climate
	1pctCO2-bgc	36-150	11	Biogeochemically-only	Long-term, CO_2 fertilization
	ssp585-bgc	2015-2100	7	Biogeochemically-only	Long-term, CO_2 fertilization
ScenarioMIP	historical	1750-2014	11	Coupled	Inter-annual variability (IAV)
	ssp585	2015-2100	11	Coupled	Inter-annual variability (IAV)

Zonal statistics computed within the Amazon basin and presented throughout the results are obtained by considering the grid-cells confined within the Amazon basin shapefile, available from the SO HYBAM service (INPE, 2019, https://hybam.obs-mip.fr/).

The ESMs performances in representing ENSO properties, the Amazon climatology, carbon and energy fluxes are evaluated against observational and quasi-observational products, and are reported in Figure S1-S4. HadISST dataset is used for assessing ESMs sea surface temperatures (Rayner et al., 2003), while ERA5 and ERA5-Land products are used to validate temperature, precipitation and soil moisture (Hersbach et al., 2020; Muñoz-Sabater et al., 2021). Finally, the FLUXCOM-RS+METEO dataset, specifically the one forced with the WFDEI meteorological dataset (Weedon et al., 2014), is used as a reference for both carbon fluxes (GPP, NEP, Total Ecosystem Respiration, TER) and energy fluxes (shortwave incoming radiation) (Jung et al., 2019, 2020).

To evaluate ESMs against the reanalysis products, as well as to compute multi-model means across variables, a conservative remapping algorithm is applied to all the data to get a regular 1° longitude x 1° latitude grid, with the exception of SST from ESMs with a curvilinear grid (Table SI1), for which a distance weighted (nearest-neighbor) average remapping is applied. The validation procedure refers to the climatological period 1979-2013. When comparing the carbon fluxes from ESMs with FLUXCOM data, the total ecosystem respiration is obtained by summing the contributions of Ra and Rh. An overview of the ESMs evaluation performances is available in the supplementary material (Figures S1-S4).

2.2 Long-term mean-state climatic effects

Increasing trends of atmospheric CO2 concentrations affect terrestrial carbon sinks directly through a fertilization effect on vegetation (carbon-concentration feedback) and indirectly by forcing changes in the physical climate via a strengthened greenhouse effect, which in turn affects vegetation (carbon-climate feedback). A common approach to disentangle the two effect relies on the carbon-cycle feedback framework, by which it is possible to estimate the magnitude of the carbon-

concentration feedback and the carbon-climate feedback (Jones et al., 2016; K. Arora et al., 2020). The contribution of these two feedbacks is estimated with the following linear equations:

$$\beta = \frac{\Delta NBP_{cum,BGC}}{\Delta ppm_{BGC}} \tag{1}$$

$$\gamma_T = \frac{\Delta NBP_{cum,RAD}}{\Delta T_{RAD}}; \quad \gamma_{mrso} = \frac{\Delta NBP_{cum,RAD}}{\Delta mrso_{RAD}}; \quad \gamma_{SW_{in}} = \frac{\Delta NBP_{cum,RAD}}{\Delta SWin_{RAD}} \tag{2}$$

Carbon sink is represented here by cumulative NBP, whose long-term sensitivity to CO_2 ppmv (β), and climate (γ), is estimated from biogeochemically only coupled simulations (1pctCO_2-bgc and ssp585-bgc) and radiative only coupled simulations (1pctCO_2-rad and ssp585-rad) respectively. Within the former, the increased CO_2 atmospheric concentration is uniquely exerting a biogeochemical effect which interests the terrestrial and ocean carbon cycle processes, whereas in the radiative simulation only the radiative transfer processes in the atmosphere are affected by the changing atmospheric CO_2 concentrations, with no consequences for biochemical processes (Friedlingstein et al., 2006; Jones et al., 2016). Changes are expressed with respect to the first year of the simulations; for 1pctCO_2 experiments only the years with atmospheric CO_2 ranges similar to the ssp585 scenario (400-1135 ppmv, resulting in 104 years) have been considered. Lastly, the carbon-climate feedback has been computed with respect to surface atmospheric temperatures (T), whereas the carbon sink sensitivity to soil moisture (mrso) and shortwave incoming radiation (SWin) is used to represent the variety of mean-state climatic changes affecting the cumulative carbon fluxes within the Amazon basin.

2.3 Carbon fluxes sensitivity at inter-annual timescales

We further assessed the sensitivity of carbon fluxes within the Amazon basin at interannual timescales, to explore the short-term variability contribution of different climatic factors. With this respect, two additional analysis have been performed. A first one aimed at assessing the relative contribution of temperature, soil moisture and shortwave-incoming radiation on NBP, GPP, Ra and Rh by adopting a multivariate predictive regression model as in the following equation, for every ESMs considered:

$$\Delta NBP = \frac{\delta NBP}{\delta T} * \Delta T + \frac{\delta NBP}{\delta mrso} * \Delta mrso + \frac{\delta NBP}{\delta SW_{in}} * \Delta SW_{in} + \epsilon \tag{3}$$

Temperature, soil moisture and shortwave incoming radiation have been chosen because of their primary control on carbon fluxes interannual variability (Jung et al., 2017). We used soil-moisture rather than precipitation as a proxy for water availability due to its stronger control on terrestrial carbon fluxes (Humphrey et al., 2018). We acknowledge that latent heat fluxes could partially contribute to interannual NBP variability by influencing vapor pressure deficit (VPD), which in turn

affects NBP. However, we decided to exclude this factor from our framework (equation 3) because transpiration, which is

180 regulated by stomatal conductance, impacts both NBP and latent heat fluxes, likely introducing correlation between them.

All the variables considered have been averaged over the calendar year, as the focus of the analysis is on interannual variability. The dependent variable (NBP, as well as GPP, Ra and Rh) has been linearly detrended to remove the influence of CO_2 fertilization and other long-term climatic changes, while the three independent variables have been detrended and standardized (subtracting the mean and dividing by their standard deviation) to obtain comparable coefficients. Therefore, the standardized

185 coefficients represent the quantitative contribution of temperature, soil-moisture and shortwave incoming radiation considering the simultaneous confounding impacts of the other variables. Specifically, a 5-fold cross-validation ridge regression model has been adopted, due to the penalty score in the cost function of ridge regression that helps to account for the collinearity among the predictors themselves. The cross-validation procedure entailed a randomized split of the dataset into training set (80%) and validation set (20%), and allowed for the selection of the best performing regularization parameter among a set of values

190 spaced evenly on a log scale. The multivariate model derives from the Scikit-Learn package, available for the Python scripting language (Pedregosa et al., 2012).

Given the predominant modulation of carbon fluxes IAV within the Amazon basin by means of ENSO (Mcphaden et al., 2021a), a further analysis is conducted to assess the ENSO contribution to Amazon vegetation productivity mediated by either

195 temperature and water-availability (using soil moisture as a proxy). For this, an annual time series of ENSO is obtained for each historical and ssp585 realization by averaging the corresponding monthly Nino3.4 index over the calendar year. The Nino3.4 index is defined as the 5-month moving average of mean sea-surface temperatures over the region 170-120°W and 5°S-5°N, subsequently detrended by means of a 1st order polynomial to remove the warming trend of SST. By taking the univariate sensitivities of temperature and soil-moisture to ENSO, and accounting for the partial derivatives of NBP with

200 respect to temperature and soil-moisture as in Equation 3, we estimate the contribution of ENSO driven by the two mechanisms as below:

$$\delta NBP_{n34}^{T} = \frac{\delta NBP}{\delta T} * \frac{dT}{dn34} \tag{4}$$

$$\delta NBP_{n34}^{mrso} = \frac{\delta NBP}{\delta mrso} * \frac{dmrso}{dn34} \tag{5}$$

205

Using the partial derivatives $\frac{\delta NBP}{\delta T}$ and $\frac{\delta NBP}{\delta mrso}$ ensures that the effects of temperature and soil moisture are considered independently, accounting for potential confounding influences from each other, a condition not met if the univariate estimates $\frac{dNBP}{dT}$ and $\frac{dNBP}{dmrso}$ were applied. A Mann-Whitney U-test of independence with Bonferroni correction was used to assess whether the zonal values of the regression coefficients within the Amazon basin are significantly different between the

7

historical period and ssp585 scenario. To mitigate the risk of overstating the significance of the statistical tests conducted, we employ a false discovery rate (FDR) control method based on (Wilks, 2016). This approach effectively addresses the issue of multiple hypothesis testing, ensuring a more accurate interpretation of the obtained results.

3 Results and Discussion

3.1 Intermodel uncertainties of carbon and climatic drivers

Amazon basin vegetation productivity and climatology shows substantial overlap across models during the historical period but strongly diverging trends across models during the ssp585 scenario, with individual models differing in magnitude and sign of projected changes (Figure 1a). The multi-model ensemble yields a cumulative NBP mean by the end of the 21st century of 59.3 ± 62 gCm^{-2}. Considering the projections of cumulative carbon sink in Figure 1a and carbon fluxes in Figure S5, the inter-model uncertainty is much higher compared to intra-model uncertainty (which stems from the intrinsic climatic variability expressed in each realization and is represented by the ± 1 standard deviation spread in Figure 1 and Figure S5). For the physical variables in Figure 1b-e, intra-model uncertainty is considerably higher than for carbon fluxes and reflects the substantial internal climate variability intrinsic in each simulation. These considerations already highlight that part of the divergence across carbon cycle predictions is related to differences in the land sensitivity to climatic forcings, rather than uncertainties in the evolution of the climate itself. Overall, the climatological variables present a stronger agreement and coherence in the sign of projected changes among ESMs with respect to NBP. A multi-model mean reduction of -21.13 mm month^{-1}, -128.93 kgm^{-2} is projected for precipitation and soil moisture, respectively (Figure 1c,d), while an increase is observed for temperature and incoming shortwave radiation (+7.08 °C and +9.23 Wm^{-2}, respectively, Figure 1b,e). Still, the multi-model ensemble spread at the end of the 21st century remains substantial for all these variables. Differences among models of one or even two orders of magnitude could be seen for instance between MRI-ES2L and CanESM5 for shortwave incoming radiation or for MIROC-ES2L and IPSL-CM6A-LR regarding soil moisture projections.

For some models, divergent NBP projections cannot be easily attributed to similar deviations in the individual climatic drivers. For instance, ACCESS-ESM1-5 and NorESM2-LM projects similar end-of-the-century temperature and soil-moisture changes, but strongly diverging trends of cumulative NBP.
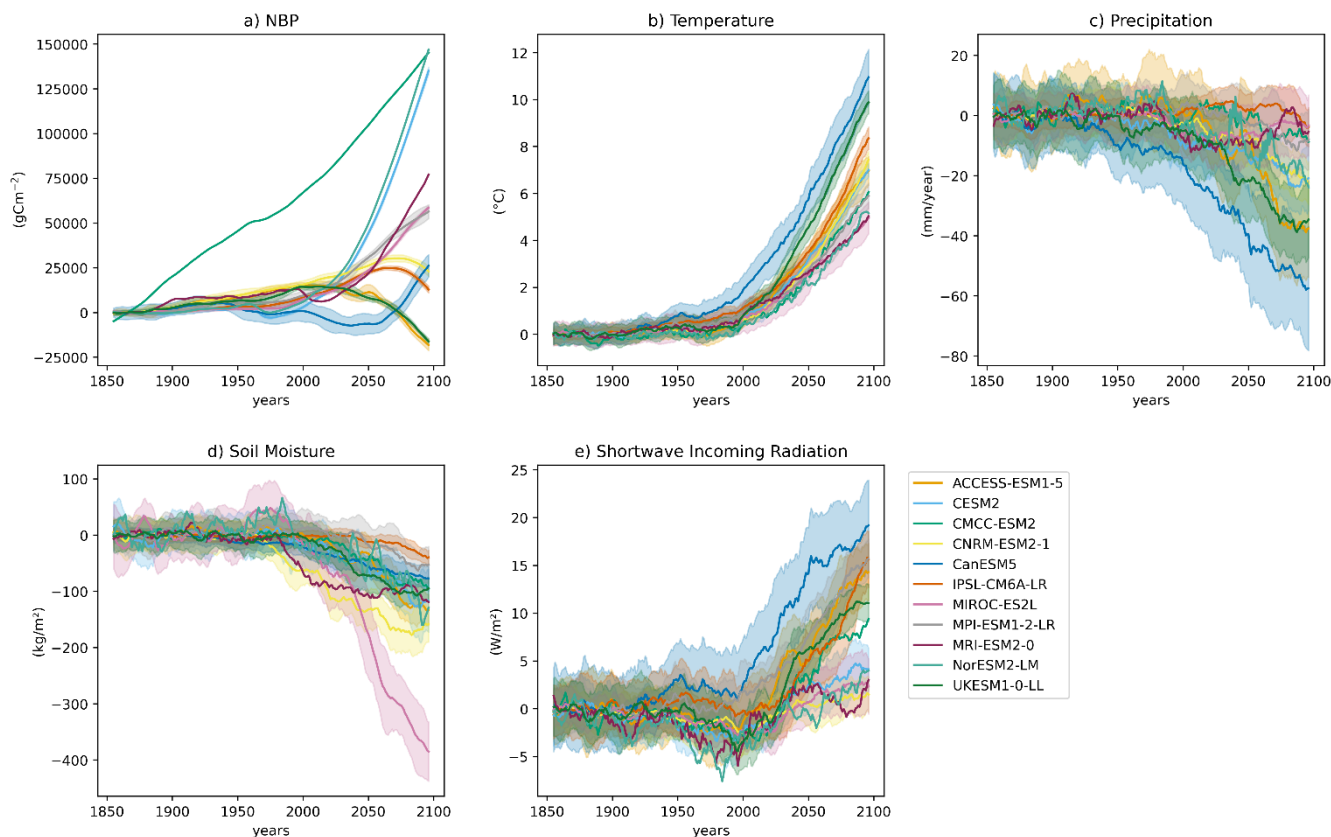
Figure 1: Long-term trends of (a) cumulative NBP, (b) temperature, (c) precipitation, (d) soil-moisture, (e) shortwave incoming radiation in the Amazon basin for the historical and ssp585 experiments. Trends are computed with respect to the first 30-year mean of the historical period (1850-1880), and are visualized as a 10-year moving average for clarity. For the models with more than one realization, both the model-ensemble mean (line) and the spread (±1 standard deviation, shading) are shown.

Regarding the intra-model spread, the highest influence of internal climatic variability (±1 standard deviations) is observed in precipitation and shortwave incoming radiation, followed by soil-moisture (spreads in Figure 1c,e and d). This indicates that within the Amazon basin, the major source of uncertainty deriving from internal climate variability is associated with cloud formation and coverage, which is causally linked with the amount of precipitation (thus soil moisture content) and shortwave incoming radiation within the regional domain. All the carbon fluxes from which NBP is derived (GPP, Ra and Rh) depict an increasing trend throughout the 21st century (Figure S5), with the notable exception of GPP and heterotrophic respiration for ACCESS-ESM1-5. Among these carbon fluxes, Rh presents the highest end of 21st century normalized uncertainty (186.74 gCm^{-2}, z-score std-dev of 1.62), followed by GPP and Ra (753.59 and 548.71 gCm^{-2}, z-score std-dev of 1.12 and 0.76 respectively). This shows that uncertainty in cumulative NBP does not solely stem from uncertainty in single climatic factors; instead, it arises from inconsistencies and differences in how models represent photosynthetic activity, autotrophic and heterotrophic respiration. Overall, inconsistencies in projected Amazon NBP cannot be simply understood as a consequence

9

of discrepancies in the climatic factors affecting vegetation, as discussed already by Heavens et al., (2013) . A point that deserves attention is therefore how the projected carbon sink in the Amazon basin is sensitive to mean-state changes in environmental drivers and climatic variability at the interannual timescale.

3.2 Long-term carbon sink sensitivity

By applying the carbon-cycle feedback framework (see Methods), the net carbon sink (cumulative NBP) response is explained by the factor β (CO$_2$ fertilization) and by the factor γ (climate effect). The net carbon sink trend driven uniquely by the CO$_2$ fertilization effect and climate is reported in Figure S6a and Figure S6b, respectively, where the consistent agreement across ESMs on the direction of the projected land carbon response to these two factors is evident.. The spatial magnitude of β derived from the 1pctCO$_2$-bgc simulation is showed in Figure S7. Most of the ESMs project a strong CO$_2$ fertilization effect within the Amazon basin for the range of atmospheric CO$_2$ concentrations of the ssp585 scenario, despite considerable variability could be observed across the models. CESM2 and NorESM2-LM present the higher vegetation sensitivity to atmospheric CO$_2$, reasonably due to the fact that both the models share the same land module CLM5 (Table S1). CMCC-ESM2 also presents high β values, but these are restricted to the most forest-dense pixel cells, as it is clear from the sharp decline in the southern and south-eastern part of the basin, a pattern which is even more drastic in ACCESS-ESM1-5.

The carbon cycle feedback framework entails to describe the positive carbon-climate feedback considering uniquely surface air temperature (γ_T), which is therefore considered as an overall representation of long-term climate impacts, as shown in Figure 2. We additionally focus on different explainable variables as equivalent terms representing long-term climate impacts (γ_{mrso} and γ_{SWin}). Thus, despite γ_T, γ_{mrso} and γ_{SWin} are not to be intended as cumulative long-term impact coefficients, the values of their standardized coefficients are reported in Figure S8 with the purpose of providing a quantitative comparison of the ESMs sensitivity to diverse climatic factors. Remarkable negative effects on Amazon carbon sink are associated with long-term increasing temperatures, and partially with less intensity, with rising trends in shortwave incoming radiation. The positive co-variability of the carbon sink with soil-moisture is almost specular of the cumulative NBP sensitivity to shortwave incoming radiation, a consequence of the strong inverse correlation among the two factors, reflecting a reduction of cloud coverage and precipitation in the Amazon basin with increasing atmospheric CO$_2$ and climate warming.

Consequently, the long-term cumulative NBP for the 1pctCO$_2$ scenario is reconstructed by means of its sensitivity to mean-state changes of temperature and atmospheric CO$_2$ and is reported in Figure 2. These results emphasize that CO$_2$ fertilization effects on vegetation productivity are expected to dominate and overcome the negative temperature influence on the long-term carbon sink evolution in the ssp585 scenario.
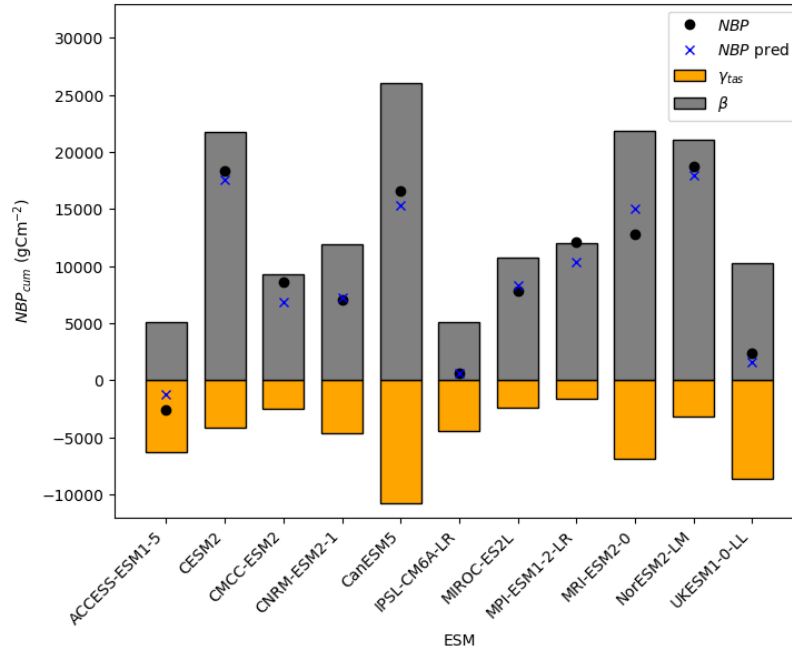
Figure 2: Contribution of carbon-concentration (β) and carbon-climate feedbacks (γ_T) to net carbon sink projections at the end of the 1pctCO2-bgc and 1pctCO2-rad simulations. Black dots represent the net cumulative NBP resulting from the arithmetic sum of cumulative NBP from 1pctCO$_2$-bgc and 1pctCO$_2$-rad simulations, whereas the blue crosses are the result of the arithmetic sum of the estimated cumulative NBP by adopting the univariate $\boldsymbol{\beta}$ and $\boldsymbol{\gamma_T}$ coefficients. Values are averaged within the Amazon basin domain.

Regarding the differences across ESMs, these discrepancies in the long-term climate-driven trend of net carbon sink in the Amazon region emerge from a very strong correlation between its sensitivity to soil-moisture γ_{mrso} and temperature γ_T, as reported in Figure 3 and Figure S9 for both 1pctCO2-rad and ssp585-rad simulations. Therefore, the Amazon carbon sensitivity to long-term climatic changes is not only discernible in the negative temperature effect, but it is also found in the positive influence to soil-moisture, indicating that the land modules of the ESMs are similarly sensitive to both the factors, despite with an inverse relationship. Additionally, temperature emerges as playing a slightly stronger role in describing the variations of carbon sink response across the different ESMs compared to soil moisture (R^2 coefficient of 0.85 vs 0.71, as illustrated in Figure 3a and Figure 3b).
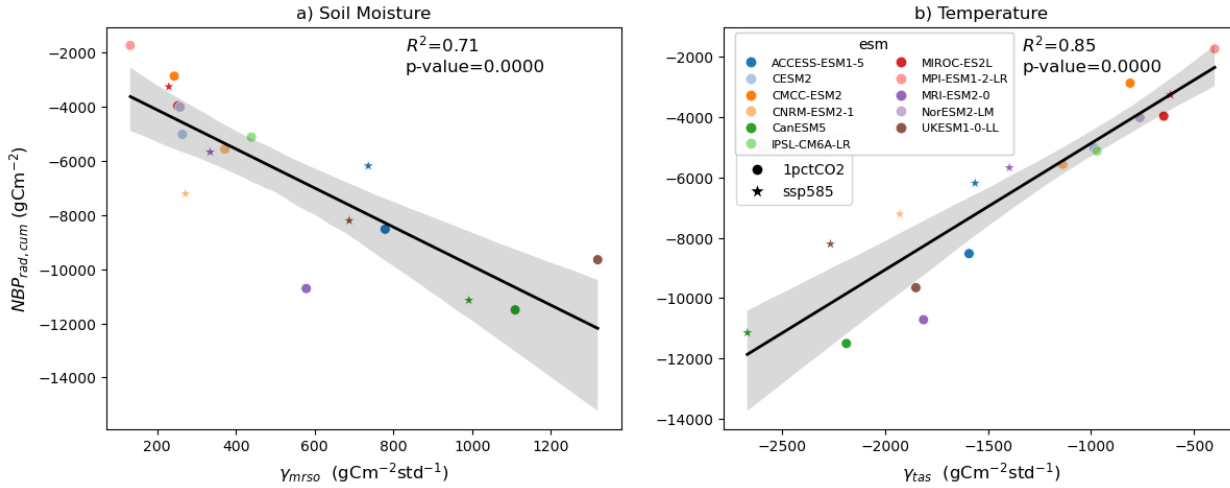
Figure 3: Intermodel uncertainty in climate-driven cumulative NBP (y-axis) as explained by differences in ESMs representation of temperature (γ_{tas}) and soil moisture (γ_{mrso}) impacts in 1pctCO2-rad and ssp585-rad simulations. The reported values are the zonally averaged within the Amazon basin geographical domain.

3.3 Inter-annual variability of carbon fluxes

Amazon carbon sink variability on shorter (interannual) timescales is assessed for the historical and ssp585 scenario considering the modulation of temperature, soil moisture and shortwave incoming radiation anomalies using a multi-linear ridge regression predictive model (see Methods). The skills of the model optimized with the 5-fold cross-validation procedure are reported in Figure S10. Overall, a multi-model mean coefficient of determination of 0.55 is obtained, despite with substantial differences across ESMs. Remarkably lower values of variance explained ($R^2<0.4$) are found for CESM2, CMCC-ESM2 and NorESM2-LM, whereas CanESM5, MIROC-ES2L and UKESM1-0-LL stand out as the models with the highest goodness of fit and predictive capability ($R^2>0.6$) (Figure S10a). Undoubtedly, we acknowledge the limitations that arise from the adoption of a linear ridge regression model. As we didn't account for interactive and non-linear effects among the predictors influencing NBP IAV, we are not able to capture a portion of the unexplained variance in our regression model. The results in Figure S10 reflects this fact, suggesting that other factors, as well as the effects emerging from the interaction of temperature, soil-moisture and shortwave incoming radiation, are likely having an important influence on NBP IAV, especially for CESM2, NorESM2-LM and partly CMCC-ESM2. Nevertheless, we opted for this modelling framework, as it still allows our results to be compared with prior works (Humphrey et al., 2018; Jung et al., 2017).
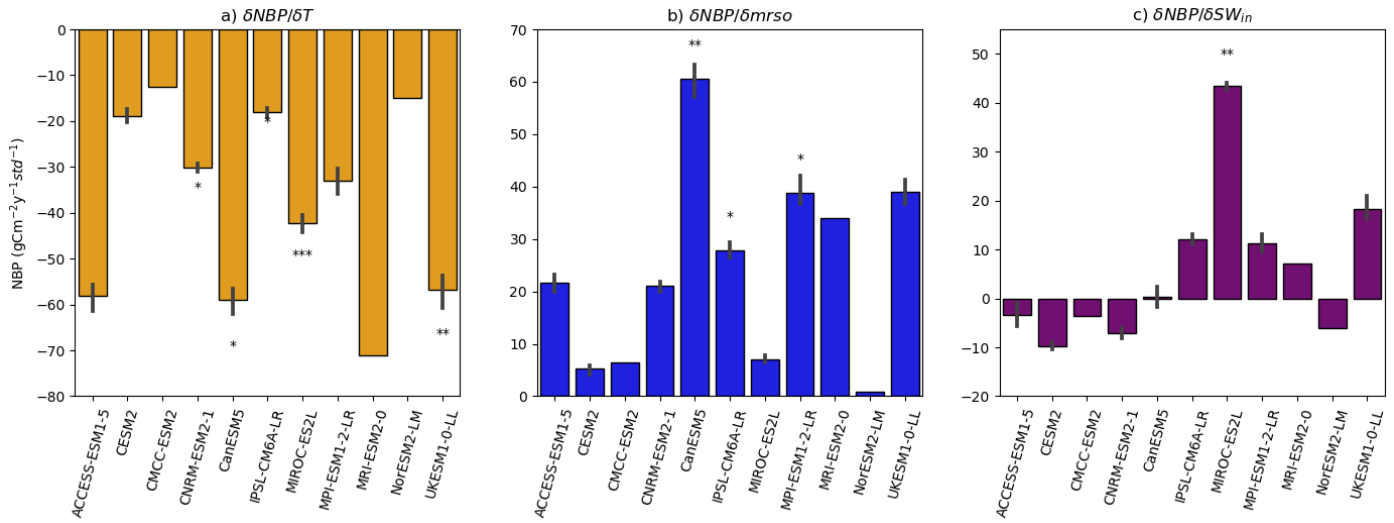
12

Figure 4: Partial derivatives explaining the contribution of temperature (a), soil moisture (b) and shortwave incoming radiation (c) to interannual NBP, averaged across the Amazon basin. The black vertical bars represent the spread in the predictors coefficients for models with more than one realization available, whereas the stars indicate the level of significance (p-value), averaged over the Amazon basin, associated to every coefficient. Statistical significance refers to the following convention: *: $1.00e\text{-}02 < p <= 5.00e\text{-}02$; **: $1.00e\text{-}03 < p <= 1.00e\text{-}02$; ***: $1.00e\text{-}04 < p <= 1.00e\text{-}03$; ****: $p <= 1.00e\text{-}04$

The relative importance of the three variables in explaining the NBP interannual variability is reported in Figure S11 for both the historical period (panel a) and the ssp585 scenario (panel b), revealing the dominant regulation of temperature for all the ESMs except CanESM5, IPSL-CM6A-LR and MPI-ESM1-2-LR, that have primarily a soil-moisture driven variability and MIROC-ES2L, which stands out for the particularly high variance explained by shortwave incoming radiation and the low contribution of soil-moisture. As will be discussed later in the next section, temperature modulation is expected to be particularly predominant in the ssp585 scenario (Figure S11b), intensified by climate change. Similar consideration can be drown by observing the standardized coefficients estimated for NBP. Those, reported for the ssp585 scenario in Figure 4, point to an intermodel qualitative agreement with respect to the contribution of temperature (negative effect) and soil-moisture (positive effect), despite with remarkable differences in the magnitude of the drivers contribution. Lower net carbon sink variability, on the other hand, is associated with shortwave incoming radiation, with ESMs diverging on the sign of the partial derivative (Figure 4c).

Similar results are found for the multilinear regression estimation in the historical period: compared to this, a general increase in the sensitivity is found for temperature and soil moisture effects in the ssp585 scenario (Figure S12), mainly a consequence of increased future interannual NBP variability. In Figure 4, seven out of eleven models project temperature as the first NBP predictor, while for CanESM5, IPSL-CM6A-LR and MPI-ESM1-2-LR soil moisture results to be more important, and MIROC-ES2L predicts shortwave incoming radiation as the most dominant driver of NBP IAV. Overall, these results complement and partially confirm what shown in a recent research (Padrón et al., 2022), which found temperature to be more

340   important than soil moisture to explain interannual variability of NBP in an ensemble of models, considering the ssp126 low

emission scenario.

The spatially explicit multi-model ensemble coefficients for NBP are reported in Figure 5, with hatches delimiting those pixel

cells where eight out of eleven ESMs agree in the sign of the partial derivative. Temperature impacts are particularly evident

in the northern part of the Amazon, whereas the positive influence of soil moisture presents high agreement almost everywhere

345   with the exception of the north western part of the basin. Considering the almost specular multi-model agreement in the positive

value of shortwave incoming radiation coefficients in that specific domain, this could reflect that the majority of the ESMs

present an energy limited regime in the area, with shortwave incoming radiation (rather than water availability) being the main

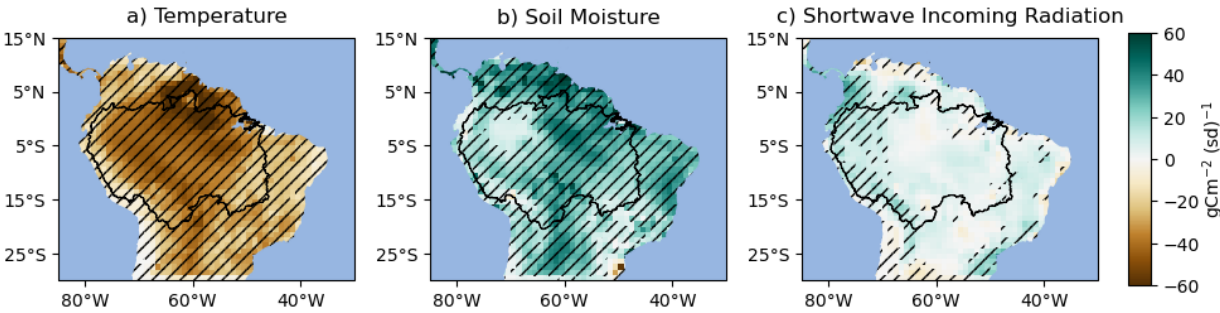limiting factor constraining ecosystem productivity at interannual timescales.

350

Figure 5: Multi model ensemble mean of the coefficient values for the climatic drivers obtained by the multi-linear regression, for the ssp585 scenario. Hatches represent those grid cells for which at least 8 out of 11 ESMs agree in the sign of the predictor value. The Amazon basin, obtained from the SO HYBAM service (https://hybam.obs-mip.fr/), is also represented.

As observed for long-term effects in Figure 3, the intermodel differences in the projection of net carbon sink variability at

355   interannual timescales are characterized by an inverse relationship between temperature and soil moisture influence: high NBP

interannual variability (expressed as NBP standard deviation, y-axis in the panels of Figure S13) is driven by lower temperature

(Figure S13a) and higher soil moisture contributions (Figure S13b).

We then identify the physical processes associated with net carbon sink that exhibits the greatest uncertainty by analysing the

variability in the estimated coefficients for each dependent variable (NBP, GPP, Ra and Rh), reported in Table 2.

360   In this procedure, the coefficients obtained from the multivariate regression model have been further standardized by dividing

each coefficient by the standard deviation of its corresponding dependent variable, ensuring a fair comparison both across

models and for the different dependent variables.

365

Table 2: Inter-model uncertainty within the Amazon basin, expressed as standard deviation. of the partial derivative values across all the ESMs. Rows represent the partial derivatives of temperature, soil moisture and shortwave incoming radiation, with respect to the dependent variables reported in the columns (carbon fluxes).

	NBP	GPP	Ra	Rh
$\dfrac{\delta Carbon}{\delta T}$	0.14	0.15	0.34	0.42
$\dfrac{\delta Carbon}{\delta mrso}$	0.24	0.25	0.31	0.45
$\dfrac{\delta Carbon}{\delta SW_{in}}$	0.28	0.36	0.30	0.30

370 The high disagreement in the sign of the shortwave incoming radiation coefficients found for NBP (panel c in Figure 4) originates from GPP sensitivity to shortwave incoming radiation $\frac{\delta GPP}{\delta SW_{in}}$ (Figure S14). Uncertainties in net carbon sink projections across ESMs therefore arise, on the one hand, mainly from differences in photosynthesis modulation by light availability. On the other hand, heterotrophic respiration sensitivity to soil moisture and temperature represents another prominent source of uncertainty across ESMs (see also panel a, b in Figure S15 showing the disagreement across ESMs

375 coefficients), whereas autotrophic respiration shows median contributions to net carbon sink uncertainty (Table 2 and Figure S16).

3.4 ENSO modulation

Given the predominant role of large-scale climatic modes of variability in influencing local climate and carbon cycle, the NBP

380 response to ENSO has been investigated. ENSO is the most important climatic mode affecting and modulating net tropical carbon sink variability at interannual timescales, and changes in key properties of ENSO could significantly impact the Amazon basin region. For example, an increase in the frequency or in the magnitude of El Niño and La Niña events under global warming, a possibility explored in previous studies (Berner et al., 2020; Brown et al., 2020; Cai et al., 2014, 2015; Fredriksen et al., 2020), could have important implications especially for the Amazon ecosystem due to a stronger inhibition

385 of the boreal winter southward shift of Inter Tropical Convergence Zone (ITCZ) that regulates the ENSO tropical teleconnection pathway. Another ENSO property that could influence the Amazon carbon cycle is the spatial location of SST anomalies in the tropical Pacific, resulting in the distinction between Central Pacific (CP) and the Eastern Pacific (EP) ENSO events (Mcphaden et al., 2021b). This spatial diversity in ENSO have been shown to have different impacts on GPP and NEP in many regions of the world, especially in the Amazon basin (Dannenberg et al., 2021), and some studies have also shown

390 that CP El Niños are projected to be more frequent under 21st century warming (e.g., Shin et al., 2022). However, the

consideration of these ENSO properties lie outside the domain and the purpose of the present research, and we leave it for future studies.

The ESMs in the considered ensemble largely overestimate the observed ENSO amplitude in the interannual-to-decadal band, with the associated spectra typically featuring a narrow peak around the 3-year periodicity (Figure S17). The ESMs also yield a diversity of changes in ENSO spectral characteristics under the warming scenario: generally, all the models represents a shift of ENSO signal toward higher frequencies, with weaker amplitude at decadal time scales and stronger amplitude at interannual time scales (Figure S17). Changes in the amplitude of the ENSO signal, represented by the Nino3.4 index standard deviation, between the ssp585 scenario (orange dots) and the historical period (light-green dots) are shown in Figure S18. Nine out of eleven ESMs show an increased ENSO variability under the ssp585 scenario, whereas CESM2 do not project any relevant changes, and UKESM1-0-LL predicts a slight decrease in ENSO amplitude.

We estimate the NBP variability related to ENSO by considering both the sensitivity of NBP to temperature and soil moisture, as well as the sensitivity of temperature and soil moisture to the Nino3.4 signal (see Methods), thus allowing to decompose the impacts associated to the two different mechanisms. The results are showed in Figure 6. First, all the models represent larger carbon sink losses related to temperature-driven anomalies compared to soil moisture ones. Second, temperature and soil moisture impacts driven by ENSO are expected to increase in magnitude during the future ssp585 scenario compared to the historical period, with the increase in δNBP_{n34}^{T} and appearing to be statistically significant for all the models but MPI-ESM1-2-LR and NorESM2-LM. Regarding δNBP_{n34}^{mrso}, on the contrary, most of the ESMs (seven out of eleven) project either a not-significant change, or a relatively low statistical significance (0.05<p-value<0.01). While the carbon cycle response to ENSO within the Amazon region presented here is well in agreement with previous research (Betts et al., 2020; Kim et al., 2017; Le, 2023; Le et al., 2021), our results further identify temperature as the key factor in the mechanism by which ENSO affects Amazon carbon fluxes in a high radiative forcing future scenario. Specifically, the higher temperature-mediated ENSO impacts arise from the higher (lower) co-variability observed in the ESMs between temperature (soil moisture) anomalies and ENSO, both during the historical period as well as in ssp585 projections (Figure S19). This is accentuated by the stronger response of NBP to temperature changes compared to soil moisture for the majority of ESMs, as mentioned above in Figure 4.
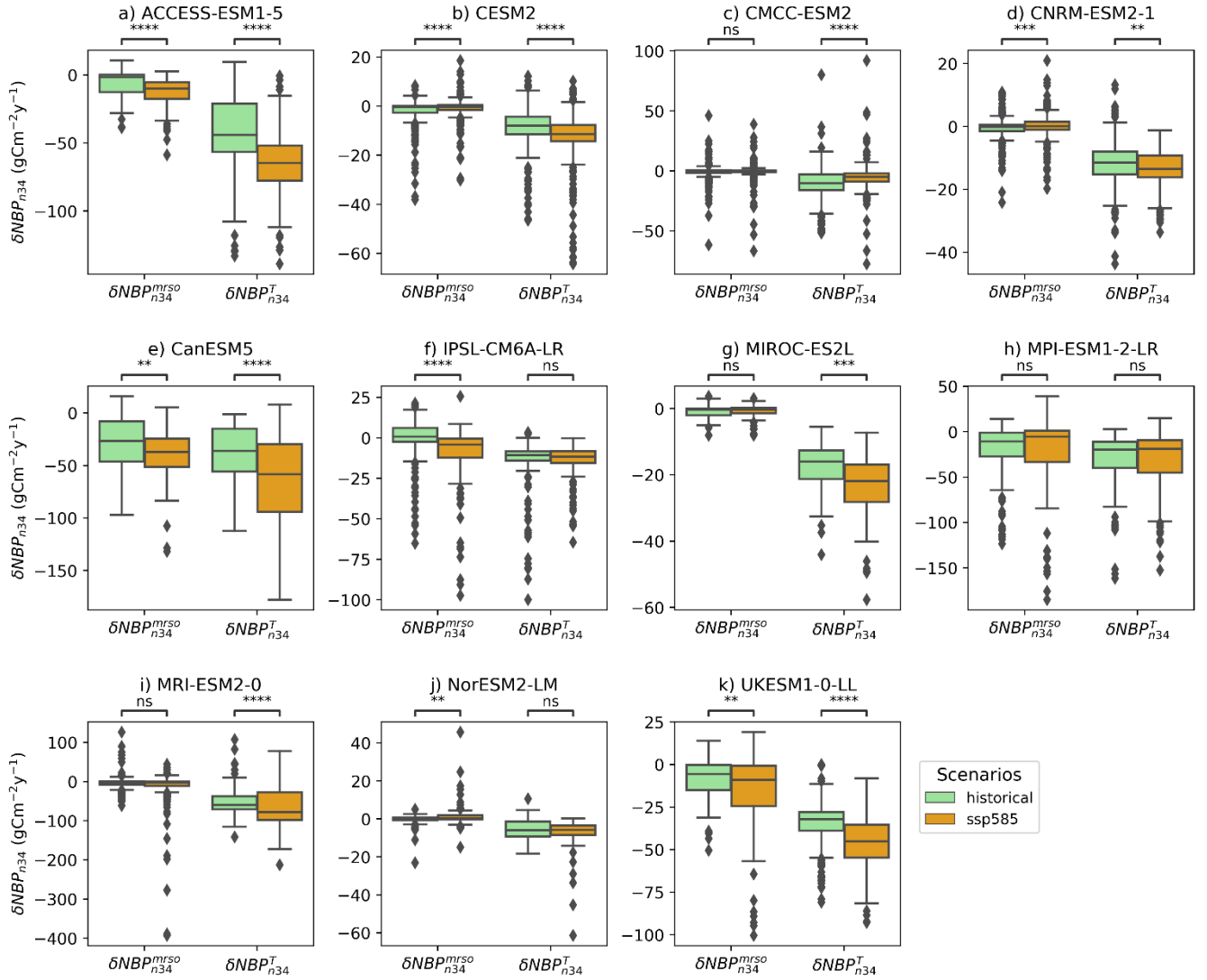
Figure 6: Variability of NBP at interannual timescales associated to ENSO (y-axis), and mediated by either soil moisture or surface air temperature (x-axis), for every ESM. Reported are the distribution of the values within the Amazon basin, for the historical period (light-green) and the ssp585 scenario (orange). Statistical difference among the distribution of the coefficients for the two periods are tested by means of a Mann-Whitney U-test and is reported in the stars above the plots with the following convention: *: $1.00e-02 < p <= 5.00e-02$; **: $1.00e-03 < p <= 1.00e-02$; ***: $1.00e-04 < p <= 1.00e-03$; ****: $p <= 1.00e-04$.

The influence of ENSO by means of temperature and soil moisture anomalies is additionally examined considering the multi-model ensemble mean of δNBP_{n34}^T and δNBP_{n34}^{mrso}. To do so, the ESMs coefficients reported in Figure 4 have been re-gridded to a common 1x1 grid using bilinear interpolation. As discernible from Figure 7, the temperature-driven impacts of ENSO are expected to be clearly stronger in the future ssp585 scenario compared to the historical period (panel a), as well as with respect to soil moisture driven impacts (panel b). Considering that climatic variability associated to ENSO in the Amazon basin in not

17

expected to significantly change in the ssp585 scenario with respect to the historical simulation for all the models (Figure S19),
430   these results indicate that climate change will significantly amplify the NBP sensitivity to temperature anomalies in the Amazon, while its influence on NBP sensitivity to soil moisture anomalies will be less pronounced.
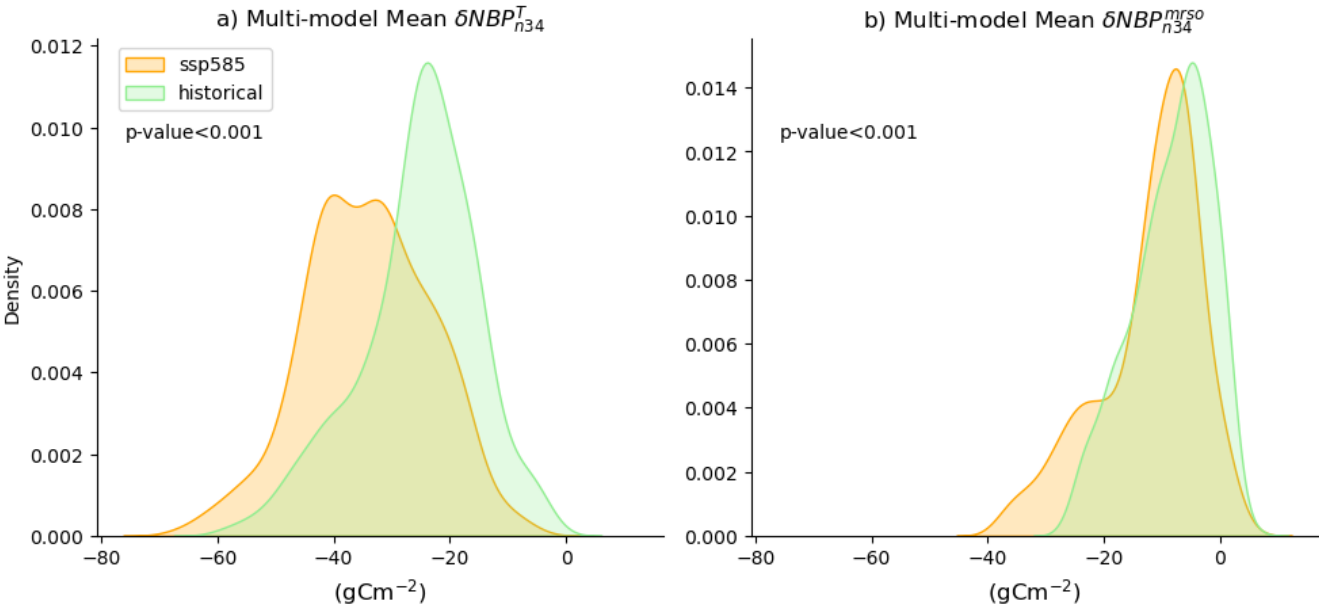

Figure 7: Only grid-cells within the Amazon basin are included. Statistical significance, tested by means of a Mann-Whitney U-test, is reported in the stars above the plot, and refers to the following convention: *: $1.00e\text{-}02 < p <= 5.00e\text{-}02$; **: $1.00e\text{-}03 < p <= 1.00e\text{-}02$; ***: $1.00e\text{-}04 < p <= 1.00e\text{-}03$; ****: $p <= 1.00e\text{-}04$

440

4 Conclusions

In conclusion, in this study we assessed the main environmental drivers affecting the long-term and IAV projections of Amazon basin carbon sink under the ssp585 high radiative forcing scenario with respect to eleven CMIP6 ESMs. Several important outcomes have been identified and confirmed.

Specifically, we recognised CO_2 fertilization as the predominant mechanism determining the long-term Amazon carbon sink trend and uncertainty under the range of atmospheric CO_2 concentrations of the ssp585 scenario (400-1135 ppmv). These results reaffirm, for the CMIP6 generation of ESMs, what reported in a previous study by Huntzinger et al. (2017), that under different research assumptions showed the predominant role of vegetation sensitivity to CO_2 in shaping the net carbon sink variability across CMIP5 generation Land Surface Models (LSMs). Additionally, we disentangled the fundamental physical processes behind net carbon sink discrepancies across ESMs, highlighting dominant mechanisms affecting simulated carbon fluxes uncertainty for the Amazon basin ecosystem. Particularly, we show that the ensemble divergence of NBP under future warming scenario is largely determined by GPP modulation by shortwave incoming radiation and uncertainty in the representation of heterotrophic respiration sensitivity to both soil moisture and temperature. Our multi-model ensemble approach expands the results obtained in previous researches (Ma et al., 2021) by allowing for an explicit consideration of model uncertainty. By showing the strong uncertainties across the driving factors of heterotrophic respiration, we suggest that not only ESMs differ in the positive modulation of temperature on Rh (controlled by the Q_{10} equation), but also largely disagree in the association between soil moisture and soil decomposition rates leading to respiration fluxes, as recently pointed out by Guenet et al., (2024).

Additionally, our results point towards a stronger ENSO-driven temperature impact on carbon sink anomalies for the vast majority of ESMs, compared to the effects associated with deficits in water availability. Accordingly, the CMIP6 multi-model ensemble considered shows a robust and statistically significant increase in carbon sink sensitivity to ENSO-driven temperature anomalies under global warming in the region of the Amazon basin: as a consequence, climate change is likely to significantly diminish the Amazon ecosystem capacity to function as a carbon sink, further aggravating the atmospheric CO_2 burden. This outcome highlights the critical role that global warming induced changes in the dynamics of modes of interannual variability could have on the Amazon region, thus contributing to the expanding scientific literature on the topic (see for example Le, 2023; Yan *et al.*, 2023). Overall, despite we were able to, at least partially, understand and quantify the contributions of different driving factors in affecting Amazon carbon cycle projections, important uncertainties still remain in the projections of Amazon response to global warming in CMIP6 generation of ESMs. On another note, we acknowledge some limitations affecting our study, particularly the application of a linear framework to describe interannual variability of carbon fluxes and ENSO-mediated impacts. A potential approach to overcome this limitation could be the adoption of machine-learning algorithms, able to detect non-linearities and describe the complex spatio-temporal features of the Earth system (Reichstein et al., 2019). This, together with a more up-to-date and uniform representation of vegetation physiological and

biogeochemical processes in the next generation of ESMs, will hopefully help generate more coherent and reliable projections of terrestrial carbon fluxes, helping to understand the faith of the Amazon basin under global warming scenarios.

Code availability: The code used to perform the analysis is publicly available at https://github.com/Matteo-Mastro/Amazon_CMIP6

Data availability: CMIP6 data are freely available and accessible from the ESGF repository (https://aims2.llnl.gov/search). FLUXCOM energy and carbon fluxes data are accessible from the Data Portal of the Max Planck Institute for Biogeochemistry, previous registration (https://www.bgc-jena.mpg.de/geodb/projects/Home.php). HadISST dataset is freely accessible from the MetOffice website (https://www.metoffice.gov.uk/hadobs/hadisst/data/download.html). ERA5 and ERA5-Land data are freely accessible from the Copernicus Climate Data Store (https://cds.climate.copernicus.eu/#!/home). The Amazon shapefile used for computing the spatial mean statistics is freely available from the Amazon basin water resources observation service (https://hybam.obs-mip.fr/).

Author contribution: MM designed the study with contributions and feedbacks from DZ and DP. MM developed the code and performed the analysis. MM prepared the manuscript with contributions and feedbacks from all the co-authors.

Competing interests: The authors declare that they have no conflict of interest.

References

Ahlström, A., Schurgers, G., Arneth, A., and Smith, B.: Robustness and uncertainty in terrestrial ecosystem carbon response to CMIP5 climate change projections, Environ. Res. Lett., 7, 044008, https://doi.org/10.1088/1748-9326/7/4/044008, 2012.

Baker, J. C. A., Garcia-Carreras, L., Gloor, M., Marsham, J. H., Buermann, W., da Rocha, H. R., Nobre, A. D., de Araujo, A. C., and Spracklen, D. V.: Evapotranspiration in the Amazon: spatial patterns, seasonality, and recent trends in observations, reanalysis, and climate models, Hydrology and Earth System Sciences, 25, 2279–2300, https://doi.org/10.5194/hess-25-2279-2021, 2021.

Bastos, A., Friedlingstein, P., Sitch, S., Chen, C., Mialon, A., Wigneron, J. P., Arora, V. K., Briggs, P. R., Canadell, J. G., Ciais, P., Chevallier, F., Cheng, L., Delire, C., Haverd, V., Jain, A. K., Joos, F., Kato, E., Lienert, S., Lombardozzi, D., Melton, J. R., Myneni, R., Nabel, J. E. M. S., Pongratz, J., Poulter, B., Rödenbeck, C., Séférian, R., Tian, H., Van Eck, C., Viovy, N., Vuichard, N., Walker, A. P., Wiltshire, A., Yang, J., Zaehle, S., Zeng, N., and Zhu, D.: Impact of the 2015/2016 El Niño on the terrestrial carbon cycle constrained by bottom-up and top-down approaches, Philosophical Transactions of the Royal Society B: Biological Sciences, 373, https://doi.org/10.1098/RSTB.2017.0304, 2018.

Beobide-Arsuaga, G., Bayr, T., Reintges, A., and Latif, · Mojib: Uncertainty of ENSO-amplitude projections in CMIP5 and CMIP6 models, Climate Dynamics, 56, 3875–3888, https://doi.org/10.1007/s00382-021-05673-4, 2021.

Berner, J., Christensen, H. M., and Sardeshmukh, P. D.: Does ENSO Regularity Increase in a Warming Climate?, Journal of Climate, 33, 1247–1259, https://doi.org/10.1175/JCLI-D-19-0545.1, 2020.

Betts, R. A., Burton, C. A., Feely, R. A., Collins, M., Jones, C. D., and Wiltshire, A. J.: ENSO and the Carbon Cycle, in: El Niño Southern Oscillation in a Changing Climate, American Geophysical Union (AGU), 453–470, https://doi.org/10.1002/9781119548164.ch20, 2020.

Boer, G. J. and Arora, V.: Temperature and concentration feedbacks in the carbon cycle, Geophysical Research Letters, 36, 2009.

Brienen, R. J. W., Phillips, O. L., Feldpausch, T. R., Gloor, E., Baker, T. R., Lloyd, J., Lopez-Gonzalez, G., Monteagudo-Mendoza, A., Malhi, Y., Lewis, S. L., Vásquez Martinez, R., Alexiades, M., Álvarez Dávila, E., Alvarez-Loayza, P., Andrade, A., Aragaõ, L. E. O. C., Araujo-Murakami, A., Arets, E. J. M. M., Arroyo, L., Aymard C., G. A., Bánki, O. S., Baraloto, C., Barroso, J., Bonal, D., Boot, R. G. A., Camargo, J. L. C., Castilho, C. V., Chama, V., Chao, K. J., Chave, J., Comiskey, J. A., Cornejo Valverde, F., Da Costa, L., De Oliveira, E. A., Di Fiore, A., Erwin, T. L., Fauset, S., Forsthofer, M., Galbraith, D. R., Grahame, E. S., Groot, N., Hérault, B., Higuchi, N., Honorio Coronado, E. N., Keeling, H., Killeen, T. J., Laurance, W. F., Laurance, S., Licona, J., Magnussen, W. E., Marimon, B. S., Marimon-Junior, B. H., Mendoza, C., Neill, D. A., Nogueira, E. M., Núñez, P., Pallqui Camacho, N. C., Parada, A., Pardo-Molina, G., Peacock, J., Penã-Claros, M., Pickavance, G. C., Pitman, N. C. A., Poorter, L., Prieto, A., Quesada, C. A., Ramírez, F., Ramírez-Angulo, H., Restrepo, Z., Roopsind, A., Rudas, A., Salomaõ, R. P., Schwarz, M., Silva, N., Silva-Espejo, J. E., Silveira, M., Stropp, J., Talbot, J., Ter Steege, H., Teran-Aguilar, J., Terborgh, J., Thomas-Caesar, R., Toledo, M., Torello-Raventos, M., Umetsu, R. K., Van Der Heijden, G. M. F., Van Der Hout, P., Guimarães Vieira, I. C., Vieira, S. A., Vilanova, E., Vos, V. A., and Zagt, R. J.: Long-term decline of the Amazon carbon sink, Nature 2015 519:7543, 519, 344–348, https://doi.org/10.1038/nature14283, 2015.

Brown, J. R., Brierley, C. M., An, S. I., Guarino, M. V., Stevenson, S., Williams, C. J. R., Zhang, Q., Zhao, A., Abe-Ouchi, A., Braconnot, P., Brady, E. C., Chandan, D., D'Agostino, R., Guo, C., Legrande, A. N., Lohmann, G., Morozova, P. A., Ohgaito, R., O'Ishi, R., Otto-Bliesner, B. L., Richard Peltier, W., Shi, X., Sime, L., Volodin, E. M., Zhang, Z., and Zheng, W.:

Comparison of past and future simulations of ENSO in CMIP5/PMIP3 and CMIP6/PMIP4 models, Climate of the Past, 16, 1777–1805, https://doi.org/10.5194/CP-16-1777-2020, 2020.

Cai, W., Borlace, S., Lengaigne, M., Van Rensch, P., Collins, M., Vecchi, G., Timmermann, A., Santoso, A., Mcphaden, M. J., Wu, L., England, M. H., Wang, G., Guilyardi, E., and Jin, F. F.: Increasing frequency of extreme El Niño events due to greenhouse warming, Nature Climate Change 2014 4:2, 4, 111–116, https://doi.org/10.1038/nclimate2100, 2014.

Cai, W., Wang, G., Santoso, A., Mcphaden, M. J., Wu, L., Jin, F.-F., Timmermann, A., Vecchi, G., Lengaigne, M., England, M. H., Dommenget, D., Takahashi, K., and Guilyardi, E.: Increased frequency of extreme La Niña events under greenhouse warming, 26–26, https://doi.org/10.1038/NCLIMATE2492, 2015.

Cai, W., Santoso, A., Collins, M., Dewitte, B., Karamperidou, C., Kug, J. S., Lengaigne, M., McPhaden, M. J., Stuecker, M. F., Taschetto, A. S., Timmermann, A., Wu, L., Yeh, S. W., Wang, G., Ng, B., Jia, F., Yang, Y., Ying, J., Zheng, X. T., Bayr, T., Brown, J. R., Capotondi, A., Cobb, K. M., Gan, B., Geng, T., Ham, Y. G., Jin, F. F., Jo, H. S., Li, X., Lin, X., McGregor, S., Park, J. H., Stein, K., Yang, K., Zhang, L., and Zhong, W.: Changing El Niño–Southern Oscillation in a warming climate, Nature Reviews Earth and Environment, 2, 628–644, https://doi.org/10.1038/s43017-021-00199-z, 2021.

Cai, W., Ng, B., Wang, G., Santoso, A., Wu, L., and Yang, K.: Increased ENSO sea surface temperature variability under four IPCC emission scenarios, Nature Climate Change 2022 12:3, 12, 228–231, https://doi.org/10.1038/s41558-022-01282-z, 2022.

Canadell, J. G., Monteiro, P. M., Costa, M. H., Da Cunha, L. C., Cox, P. M., Alexey, V., Henson, S., Ishii, M., Jaccard, S., and Koven, C.: Global carbon and other biogeochemical cycles and feedbacks, in: Climate Change 2021: The Physical Science Basis. Contribution of Working Group I to the Sixth Assessment Report of the Intergovernmental Panel on Climate Change, Cambridge University Press, Cambridge, United Kingdom and New York, NY, USA, 673–816, 2021.

Chen, L., Li, T., Yu, Y., and Behera, S. K.: A possible explanation for the divergent projection of ENSO amplitude change under global warming, Climate Dynamics 2017 49:11, 49, 3799–3811, https://doi.org/10.1007/S00382-017-3544-X, 2017.

Dannenberg, M. P., Smith, W. K., Zhang, Y., Song, C., Huntzinger, D. N., and Moore, D. J. P.: Large-Scale Reductions in Terrestrial Carbon Uptake Following Central Pacific El Niño, Geophysical Research Letters, 48, https://doi.org/10.1029/2020GL092367, 2021.

Davidson, E. A., de Araújo, A. C., Artaxo, P., Balch, J. K., Brown, I. F., C. Bustamante, M. M., Coe, M. T., DeFries, R. S., Keller, M., Longo, M., Munger, J. W., Schroeder, W., Soares-Filho, B. S., Souza, C. M., and Wofsy, S. C.: The Amazon basin in transition, Nature, 481, 321–328, https://doi.org/10.1038/nature10717, 2012.

Eyring, V., Bony, S., Meehl, G. A., Senior, C. A., Stevens, B., Stouffer, R. J., and Taylor, K. E.: Overview of the Coupled Model Intercomparison Project Phase 6 (CMIP6) experimental design and organization, Geosci. Model Dev., 9, 1937–1958, https://doi.org/10.5194/gmd-9-1937-2016, 2016.

Fleischer, K., Rammig, A., De Kauwe, M. G., Walker, A. P., Domingues, T. F., Fuchslueger, L., Garcia, S., Goll, D. S., Grandis, A., and Jiang, M.: Amazon forest response to CO2 fertilization dependent on plant phosphorus acquisition, Nature Geoscience, 12, 736–741, 2019.

Fredriksen, H. B., Berner, J., Subramanian, A. C., and Capotondi, A.: How Does El Niño–Southern Oscillation Change Under Global Warming—A First Look at CMIP6, Geophysical Research Letters, 47, e2020GL090640-e2020GL090640, https://doi.org/10.1029/2020GL090640, 2020.

Friedlingstein, P., Cox, P., Betts, R., Bopp, L., von Bloh, W., Brovkin, V., Cadule, P., Doney, S., Eby, M., and Fung, I.: Climate–carbon cycle feedback analysis: results from the C4MIP model intercomparison, Journal of climate, 19, 3337–3353, 2006.

Gao, Q., Wang, G., Xue, K., Yang, Y., Xie, J., Yu, H., Bai, S., Liu, F., He, Z., and Ning, D.: Stimulation of soil respiration by elevated CO2 is enhanced under nitrogen limitation in a decade-long grassland study, Proceedings of the National Academy of Sciences, 117, 33317–33324, 2020.

Gentine, P., Green, J. K., Guérin, M., Humphrey, V., Seneviratne, S. I., Zhang, Y., and Zhou, S.: Coupling between the terrestrial carbon and water cycles—a review, Environmental Research Letters, 14, 083003–083003, https://doi.org/10.1088/1748-9326/AB22D6, 2019.

Green, J. K., Seneviratne, S. I., Berg, A. M., Findell, K. L., Hagemann, S., Lawrence, D. M., and Gentine, P.: Large influence of soil moisture on long-term terrestrial carbon uptake, Nature 2019 565:7740, 565, 476–479, https://doi.org/10.1038/s41586-018-0848-x, 2019.

Guenet, B., Orliac, J., Cécillon, L., Torres, O., Sereni, L., Martin, P. A., Barré, P., and Bopp, L.: Spatial biases reduce the ability of Earth system models to simulate soil heterotrophic respiration fluxes, Biogeosciences, 21, 657–669, https://doi.org/10.5194/bg-21-657-2024, 2024.

Heavens, N. G., S. Ward, D., and M. M., N.: Studying and Projecting Climate Change with Earth System Models | Learn Science at Scitable, Nat. Edu., 2013.

Hersbach, H., Bell, B., Berrisford, P., Hirahara, S., Horányi, A., Muñoz-Sabater, J., Nicolas, J., Peubey, C., Radu, R., and Schepers, D.: The ERA5 global reanalysis, Quarterly Journal of the Royal Meteorological Society, 146, 1999–2049, 2020.

Hubau, W., Lewis, S. L., Phillips, O. L., Affum-Baffoe, K., Beeckman, H., Cuní-Sanchez, A., Daniels, A. K., Ewango, C. E., Fauset, S., and Mukinzi, J. M.: Asynchronous carbon sink saturation in African and Amazonian tropical forests, Nature, 579, 80–87, 2020.

Humphrey, V., Zscheischler, J., Ciais, P., Gudmundsson, L., Sitch, S., and Seneviratne, S. I.: Sensitivity of atmospheric CO2 growth rate to observed changes in terrestrial water storage, Nature, 560, 628–631, 2018.

Huntingford, C., Zelazowski, P., Galbraith, D., Mercado, L. M., Sitch, S., Fisher, R., Lomas, M., Walker, A. P., Jones, C. D., and Booth, B. B.: Simulated resilience of tropical rainforests to CO2-induced climate change, Nature Geoscience, 6, 268–273, 2013.

Huntzinger, D. N., Michalak, A. M., Schwalm, C., Ciais, P., King, A. W., Fang, Y., Schaefer, K., Wei, Y., Cook, R. B., Fisher, J. B., Hayes, D., Huang, M., Ito, A., Jain, A. K., Lei, H., Lu, C., Maignan, F., Mao, J., Parazoo, N., Peng, S., Poulter, B., Ricciuto, D., Shi, X., Tian, H., Wang, W., Zeng, N., and Zhao, F.: Uncertainty in the response of terrestrial carbon sink to environmental drivers undermines carbon-climate feedback predictions, Sci Rep, 7, 4765, https://doi.org/10.1038/s41598-017-03818-2, 2017.

INPE, N. I. F. S. RESEARCH. E. O. G. C.: MONITORING PROGRAM OF THE AMAZON AND OTHER BIOMES., 2019.

Jiménez-Muñoz, J. C., Mattar, C., Barichivich, J., Santamaría-Artigas, A., Takahashi, K., Malhi, Y., Sobrino, J. A., and Schrier, G. V. D.: Record-breaking warming and extreme drought in the Amazon rainforest during the course of El Niño 2015–2016, Scientific Reports 2016 6:1, 6, 1–7, https://doi.org/10.1038/srep33130, 2016.

Jones, C. D., Collins, M., Cox, P. M., and Spall, S. A.: The carbon cycle response to ENSO: A coupled climate–carbon cycle model study, Journal of Climate, 14, 4113–4129, 2001.

Jones, C. D., Arora, V., Friedlingstein, P., Bopp, L., Brovkin, V., Dunne, J., Graven, H., Hoffman, F., Ilyina, T., John, J. G., Jung, M., Kawamiya, M., Koven, C., Pongratz, J., Raddatz, T., Randerson, J. T., and Zaehle, S.: C4MIP-The Coupled Climate-605 Carbon Cycle Model Intercomparison Project: experimental protocol for CMIP6, Geosci. Model Dev, 9, 2853–2880, https://doi.org/10.5194/gmd-9-2853-2016, 2016.

Jung, M., Reichstein, M., Schwalm, C. R., Huntingford, C., Sitch, S., Ahlström, A., Arneth, A., Camps-Valls, G., Ciais, P., Friedlingstein, P., Gans, F., Ichii, K., Jain, A. K., Kato, E., Papale, D., Poulter, B., Raduly, B., Rödenbeck, C., Tramontana, G., Viovy, N., Wang, Y.-P., Weber, U., Zaehle, S., and Zeng, N.: Compensatory water effects link yearly global land CO2 610 sink changes to temperature, Nature, 541, 516–520, https://doi.org/10.1038/nature20780, 2017.

Jung, M., Koirala, S., Weber, U., Ichii, K., Gans, F., Camps-Valls, G., Papale, D., Schwalm, C., Tramontana, G., and Reichstein, M.: The FLUXCOM ensemble of global land-atmosphere energy fluxes, Scientific data, 6, 1–14, 2019.

Jung, M., Schwalm, C., Migliavacca, M., Walther, S., Camps-Valls, G., Koirala, S., Anthoni, P., Besnard, S., Bodesheim, P., Carvalhais, N., Chevallier, F., Gans, F., Goll, D. S., Haverd, V., Köhler, P., Ichii, K., Jain, A. K., Liu, J., Lombardozzi, D., 615 Nabel, J. E. M. S., Nelson, J. A., O'sullivan, M., Pallandt, M., Papale, D., Peters, W., Pongratz, J., Rödenbeck, C., Sitch, S., Tramontana, G., Walker, A., Weber, U., and Reichstein, M.: Scaling carbon fluxes from eddy covariance sites to globe: synthesis and evaluation of the FLUXCOM approach, Biogeosciences, 17, 1343–1365, https://doi.org/10.5194/bg-17-1343-2020, 2020.

K. Arora, V., Katavouta, A., Williams, R. G., Jones, C. D., Brovkin, V., Friedlingstein, P., Schwinger, J., Bopp, L., Boucher, 620 O., Cadule, P., Chamberlain, M. A., Christian, J. R., Delire, C., Fisher, A. R. A., Hajima, T., Ilyina, T., Joetzjer, E., Kawamiya, M., Koven, C. D., Krasting, J. P., Law, R. M., Lawrence, D. M., Lenton, A., Lindsay, K., Pongratz, J., Raddatz, T., Séférian, R., Tachiiri, K., Tjiputra, J. F., Wiltshire, A., Wu, T., and Ziehn, T.: Carbon-concentration and carbon-climate feedbacks in CMIP6 models and their comparison to CMIP5 models, Biogeosciences, 17, 4173–4222, https://doi.org/10.5194/BG-17-4173-2020, 2020.

625 Kim, J.-S., Kug, J.-S., Yoon, J.-H., and Jeong, S.-J.: Increased Atmospheric CO2 Growth Rate during El Niño Driven by Reduced Terrestrial Productivity in the CMIP5 ESMs, Journal of Climate, 29, 8783–8805, https://doi.org/10.1175/JCLI-D-14-00672.1, 2016.

Kim, J.-S., Kug, J.-S., and Jeong, S.-J.: Intensification of terrestrial carbon cycle related to El Niño–Southern Oscillation under greenhouse warming, Nature Communications 2017 8:1, 8, 1–8, https://doi.org/10.1038/s41467-017-01831-7, 2017.

630 Kimm, H., Park, S.-W., Jun, S.-Y., and Kug, J.-S.: How Does Plant CO2 Physiological Forcing Amplify Amazon Warming in CMIP6 Earth System Models?, Earth's Future, 12, e2023EF004223, https://doi.org/10.1029/2023EF004223, 2024.

Koch, A., Hubau, W., and Lewis, S. L.: Earth system models are not capturing present-day tropical forest carbon dynamics, Earth's Future, 9, e2020EF001874, 2021a.

Koch, A., Brierley, C., and L. Lewis, S.: Effects of Earth system feedbacks on the potential mitigation of large-scale tropical 635 forest restoration, Biogeosciences, 18, 2627–2647, https://doi.org/10.5194/BG-18-2627-2021, 2021b.

Kooperman, G. J., Chen, Y., Hoffman, F. M., Koven, C. D., Lindsay, K., Pritchard, M. S., Swann, A. L. S., and Randerson, J. T.: Forest response to rising CO2 drives zonally asymmetric rainfall change over tropical land, Nature Clim Change, 8, 434–440, https://doi.org/10.1038/s41558-018-0144-7, 2018.

Koren, G., van Schaik, E., Araújo, A. C., Boersma, K. F., Gärtner, A., Killaars, L., Kooreman, M. L., Kruijt, B., van der Laan-Luijkx, I. T., von Randow, C., Smith, N. E., and Peters, W.: Widespread reduction in sun-induced fluorescence from the Amazon during the 2015/2016 El Niño, Philosophical Transactions of the Royal Society B: Biological Sciences, 373, 20170408, https://doi.org/10.1098/rstb.2017.0408, 2018.

Langenbrunner, B., Pritchard, M. S., Kooperman, G. J., and Randerson, J. T.: Why Does Amazon Precipitation Decrease When Tropical Forests Respond to Increasing CO2?, Earth's Future, 7, 450–468, https://doi.org/10.1029/2018EF001026, 2019.

Le, T.: Increased impact of the El Niño–Southern Oscillation on global vegetation under future warming environment, Sci Rep, 13, 14459, https://doi.org/10.1038/s41598-023-41590-8, 2023.

Le, T., Ha, K. J., and Bae, D. H.: Increasing Causal Effects of El Niño–Southern Oscillation on the Future Carbon Cycle of Terrestrial Ecosystems, Geophysical Research Letters, 48, e2021GL095804-e2021GL095804, https://doi.org/10.1029/2021GL095804, 2021.

Li, Y., Baker, J. C. A., Brando, P. M., Hoffman, F. M., Lawrence, D. M., Morton, D. C., Swann, A. L. S., Uribe, M. del R., and Randerson, J. T.: Future increases in Amazonia water stress from CO2 physiology and deforestation, Nat Water, 1, 769–777, https://doi.org/10.1038/s44221-023-00128-y, 2023.

Lin, S., Hu, Z., Wang, Y., Chen, X., He, B., Song, Z., Sun, S., Wu, C., Zheng, Y., Xia, X., Liu, L., Tang, J., Sun, Q., Joos, F., and Yuan, W.: Underestimated Interannual Variability of Terrestrial Vegetation Production by Terrestrial Ecosystem Models, Global Biogeochemical Cycles, 37, e2023GB007696, https://doi.org/10.1029/2023GB007696, 2023.

Liu, J., Bowman, K. W., Schimel, D. S., Parazoo, N. C., Jiang, Z., Lee, M., Bloom, A. A., Wunch, D., Frankenberg, C., Sun, Y., O'Dell, C. W., Gurney, K. R., Menemenlis, D., Gierach, M., Crisp, D., and Eldering, A.: Contrasting carbon cycle responses of the tropical continents to the 2015–2016 El Niño, Science, 358, https://doi.org/10.1126/science.aam5690, 2017.

Liu, L., Gudmundsson, L., Hauser, M., Qin, D., Li, S., and Seneviratne, S. I.: Soil moisture dominates dryness stress on ecosystem production globally, Nature communications, 11, 4892, 2020.

Liu, L., Ciais, P., Wu, M., Padrón, R. S., Friedlingstein, P., Schwaab, J., Gudmundsson, L., and Seneviratne, S. I.: Increasingly negative tropical water–interannual CO2 growth rate coupling, Nature, 618, 755–760, https://doi.org/10.1038/s41586-023-06056-x, 2023.

Ma, Y., Yue, X., Zhou, H., Gong, C., Lei, Y., Tian, C., and Cao, Y.: Identifying the dominant climate-driven uncertainties in modeling gross primary productivity, Science of The Total Environment, 800, 149518, https://doi.org/10.1016/j.scitotenv.2021.149518, 2021.

McGregor, S., Cassou, C., Kosaka, Y., and Phillips, A. S.: Projected ENSO Teleconnection Changes in CMIP6, Geophysical Research Letters, 49, e2021GL097511-e2021GL097511, https://doi.org/10.1029/2021GL097511, 2022.

Mcphaden, M. J., Santoso, A., and Cai, W.: ENSO and the Carbon Cycle, 2021a.

Mcphaden, M. J., Santoso, A., and Cai, W.: ENSO Diversity, 2021b.

Mcphaden, M. J., Santoso, A., and Cai, W.: ENSO Teleconnections, 2021c.

Muñoz-Sabater, J., Dutra, E., Agustí-Panareda, A., Albergel, C., Arduini, G., Balsamo, G., Boussetta, S., Choulga, M., Harrigan, S., and Hersbach, H.: ERA5-Land: A state-of-the-art global reanalysis dataset for land applications, Earth System Science Data, 13, 4349–4383, 2021.

675   O'Neill, B. C., Tebaldi, C., Van Vuuren, D. P., Eyring, V., Friedlingstein, P., Hurtt, G., Knutti, R., Kriegler, E., Lamarque, J. F., Lowe, J., Meehl, G. A., Moss, R., Riahi, K., and Sanderson, B. M.: The Scenario Model Intercomparison Project (ScenarioMIP) for CMIP6, Geoscientific Model Development, 9, 3461–3482, https://doi.org/10.5194/GMD-9-3461-2016, 2016.

O'Sullivan, M., Spracklen, D. V., Batterman, S. A., Arnold, S. R., Gloor, M., and Buermann, W.: Have synergies between
680   nitrogen deposition and atmospheric CO_2 driven the recent enhancement of the terrestrial carbon sink?, Global Biogeochemical Cycles, 33, 163–180, 2019.

Padrón, R. S., Gudmundsson, L., Liu, L., Humphrey, V., and Seneviratne, S. I.: Drivers of intermodel uncertainty in land carbon sink projections, Biogeosciences, 19, 5435–5448, 2022.

Pan, Y., Birdsey, R. A., Fang, J., Houghton, R., Kauppi, P. E., Kurz, W. A., Phillips, O. L., Shvidenko, A., Lewis, S. L., and
685   Canadell, J. G.: A large and persistent carbon sink in the world's forests, Science, 333, 988–993, 2011.

Park, S. W., Kim, J. S., Kug, J. S., Stuecker, M. F., Kim, I. W., and Williams, M.: Two Aspects of Decadal ENSO Variability Modulating the Long-Term Global Carbon Cycle, Geophysical Research Letters, 47, https://doi.org/10.1029/2019GL086390, 2020.

Parsons, L. A.: Implications of CMIP6 Projected Drying Trends for 21st Century Amazonian Drought Risk, Earth's Future, 8,
690   e2020EF001608-e2020EF001608, https://doi.org/10.1029/2020EF001608, 2020.

Pedregosa, F., Varoquaux, G., Gramfort, A., Michel, V., Thirion, B., Grisel, O., Blondel, M., Prettenhofer, P., Weiss, R., Dubourg, V., Vanderplas, J., Passos, A., and Cournapeau, D.: Scikit-learn: Machine Learning in Python, MACHINE LEARNING IN PYTHON, 2012.

Perry, S. J., McGregor, S., Sen Gupta, A., England, M. H., and Maher, N.: Projected late 21st century changes to the regional
695   impacts of the El Niño-Southern Oscillation, Climate Dynamics, 54, 395–412, https://doi.org/10.1007/S00382-019-05006-6/FIGURES/10, 2020.

Phillips, O. L., Aragão, L. E., Lewis, S. L., Fisher, J. B., Lloyd, J., López-González, G., Malhi, Y., Monteagudo, A., Peacock, J., and Quesada, C. A.: Drought sensitivity of the Amazon rainforest, Science, 323, 1344–1347, 2009.

Piao, S., Wang, X., Wang, K., Li, X., Bastos, A., Canadell, J. G., Ciais, P., Friedlingstein, P., and Sitch, S.: Interannual variation
700   of terrestrial carbon cycle: Issues and perspectives, Global Change Biology, 26, 300–318, https://doi.org/10.1111/GCB.14884, 2020.

Raoult, N., Jupp, T., Booth, B., and Cox, P.: Combining local model calibration with the emergent constraint approach to reduce uncertainty in the tropical land carbon cycle feedback, Earth System Dynamics, 14, 723–731, https://doi.org/10.5194/esd-14-723-2023, 2023.

705   Rayner, N. A. A., Parker, D. E., Horton, E. B., Folland, C. K., Alexander, L. V., Rowell, D. P., Kent, E. C., and Kaplan, A.: Global analyses of sea surface temperature, sea ice, and night marine air temperature since the late nineteenth century, Journal of Geophysical Research: Atmospheres, 108, 2003.

Reichstein, M., Camps-Valls, G., Stevens, B., Jung, M., Denzler, J., Carvalhais, N., and Prabhat: Deep learning and process understanding for data-driven Earth system science, Nature, 566, 195–204, https://doi.org/10.1038/s41586-019-0912-1, 2019.

Shin, N.-Y., Kug, J.-S., Stuecker, M. F., Jin, F.-F., Timmermann, A., and Kim, G.-I.: More frequent central Pacific El Niño and stronger eastern pacific El Niño in a warmer climate, npj Clim Atmos Sci, 5, 101, https://doi.org/10.1038/s41612-022-00324-9, 2022.

Uribe, M. del R., Coe, M. T., Castanho, A. D., Macedo, M. N., Valle, D., and Brando, P. M.: Net loss of biomass predicted for tropical biomes in a changing climate, Nature Climate Change, 1–8, 2023.

Walker, A. P., De Kauwe, M. G., Bastos, A., Belmecheri, S., Georgiou, K., Keeling, R. F., McMahon, S. M., Medlyn, B. E., Moore, D. J., and Norby, R. J.: Integrating the evidence for a terrestrial carbon sink caused by increasing atmospheric CO2, New phytologist, 229, 2413–2445, 2021.

Weedon, G. P., Balsamo, G., Bellouin, N., Gomes, S., Best, M. J., and Viterbo, P.: The WFDEI meteorological forcing data set: WATCH Forcing Data methodology applied to ERA-Interim reanalysis data, Water Resources Research, 50, 7505–7514, https://doi.org/10.1002/2014WR015638, 2014.

Wilks, D. S.: "The Stippling Shows Statistically Significant Grid Points": How Research Results are Routinely Overstated and Overinterpreted, and What to Do about It, Bulletin of the American Meteorological Society, 97, 2263–2273, https://doi.org/10.1175/BAMS-D-15-00267.1, 2016.

Xu, W., Chang, J., Ciais, P., Guenet, B., Viovy, N., Ito, A., Reyer, C. P. O., Tian, H., Shi, H., Frieler, K., Forrest, M., Ostberg, S., Schaphoff, S., and Hickler, T.: Reducing Uncertainties of Future Global Soil Carbon Responses to Climate and Land Use Change With Emergent Constraints, Global Biogeochemical Cycles, 34, e2020GB006589, https://doi.org/10.1029/2020GB006589, 2020.

Yan, R., Wang, J., Ju, W., Goll, D. S., Jain, A. K., Sitch, S., Tian, H., Benjamin, P., Jiang, F., and Wang, H.: Interactive effects of the El Niño-Southern Oscillation and Indian Ocean Dipole on the tropical net ecosystem productivity, Agricultural and Forest Meteorology, 336, 109472, https://doi.org/10.1016/j.agrformet.2023.109472, 2023.

Yeh, S. W., Cai, W., Min, S. K., McPhaden, M. J., Dommenget, D., Dewitte, B., Collins, M., Ashok, K., An, S. I., Yim, B. Y., and Kug, J. S.: ENSO Atmospheric Teleconnections and Their Response to Greenhouse Gas Forcing, Reviews of Geophysics, 56, 185–206, https://doi.org/10.1002/2017RG000568, 2018.

Zhang, W., Schurgers, G., Peñuelas, J., Fensholt, R., Yang, H., Tang, J., Tong, X., Ciais, P., and Brandt, M.: Recent decrease of the impact of tropical temperature on the carbon cycle linked to increased precipitation, Nat Commun, 14, 965, https://doi.org/10.1038/s41467-023-36727-2, 2023.

Zhang, Y., Dannenberg, M. P., Hwang, T., Song, C., Zhang, Y., Dannenberg, M. P., Hwang, T., and Song, C.: El Niño-Southern Oscillation-Induced Variability of Terrestrial Gross Primary Production During the Satellite Era, JGRG, 124, 2419–2431, https://doi.org/10.1029/2019JG005117, 2019.

Zheng, X.-T., Hui, C., and Yeh, S.-W.: Response of ENSO amplitude to global warming in CESM large ensemble: uncertainty due to internal variability, Climate Dynamics 2017 50:11, 50, 4019–4035, https://doi.org/10.1007/S00382-017-3859-7, 2017.

Zhu, Q., Riley, W. J., Tang, J., Collier, N., Hoffman, F. M., Yang, X., and Bisht, G.: Representing Nitrogen, Phosphorus, and Carbon Interactions in the E3SM Land Model: Development and Global Benchmarking, Journal of Advances in Modeling Earth Systems, 11, 2238–2258, https://doi.org/10.1029/2018MS001571, 2019.

Zhu, Z., Piao, S., Xu, Y., Bastos, A., Ciais, P., and Peng, S.: The effects of teleconnections on carbon fluxes of global terrestrial ecosystems, Geophysical Research Letters, 44, 3209–3218, https://doi.org/10.1002/2016GL071743, 2017.